Simultaneous Localization, Mapping and Moving-Object Tracking Using Helmet-Mounted LiDAR for Micro-Mobility

Ibuki Yoshida, Akihiko Yoshida
Graduate School of Science and Engineering
Doshisha University
Kyotanabe, Kyoto, Japan
e-mail: ctwg0157@mail4.doshisha.ac.jp

Masafumi Hashimoto, Kazuhiko Takahashi
Faculty of Science and Engineering
Doshisha University
Kyotanabe, Kyoto, Japan
e-mail: {mhashimo, katakaha}@mail.doshisha.ac.jp

***Abstract*— This paper presents a method of Simultaneous Localization, Mapping and Tracking of Moving Objects (SLAMTMO) using a Light Detection And Ranging sensor (LiDAR) mounted on a smart helmet worn by a vehicle rider. This technology can be used to active safety for micro-mobility, such as bicycles, e-bikes, and electric scooters, which are prioritized as personal commuters in the endemic society of coronavirus disease 2019. Distortion in the scan data from the LiDAR is corrected by estimating the helmet's pose (three-dimensional position and attitude angle) based on the information from Normal Distributions Transform (NDT)-based SLAM and an inertial measurement unit. The static and moving-object scan data, which originate from static and moving objects in the environments, respectively, are classified by subtracting the environment map generated by NDT-based SLAM from the LiDAR current scan data. The moving scan data are used for TMO based on a Bayesian filter, whereas the static scan data are used for point-cloud mapping. The experimental results in a road environment of our university campus show the effectiveness of the proposed SLAMTMO method.**

Keywords—helmet LiDAR; SLAM; moving-object tracking; micro-mobility.

I. INTRODUCTION

There have been numerous studies on active safety and autonomous driving in the field of Intelligent Transportation Systems (ITS) [1]. In the field of last-mile automation, there has also been a flourishing study on delivery robots [2]. The environmental map building using Simultaneous Localization And Mapping (SLAM) technology [3, 4] and Tracking of Moving Objects (TMO), such as cars, cyclists and pedestrians [5, 6], are important issues for autonomous driving and active safety of vehicles and mobile robots. Many related studies have been using cameras, radars, and Light Detection And Ranging (LiDAR). In this paper, we focus on SLAMTMO with a vehicle-mounted LiDAR.

To build a three-dimensional (3D) point-cloud map in community road environments, we presented a mapping method using car-mounted LiDAR based on Normal Distributions Transform (NDT)-Graph SLAM [7]. Using motorcycle-mounted LiDAR, we also proposed a method of 3D point-cloud mapping [8]. Moreover, we presented a TMO method utilizing car and motorcycle-mounted LiDAR [9, 10].

Coronavirus disease 2019 has caused people to be highly resistant to utilizing conventional means of urban transportation, such as crowded trains and buses. Hence, to escape the three Cs' (closed spaces, crowded spaces, and close-contact settings), the use of single-seater "micro-mobility", such as bicycles, e-bikes, electric scooters, and personal mobilities, are on the increase for short-distance travel in urban cities. The demand for micro-mobility additionally increased in the endemic society.

Even though the frequency of traffic accidents involving micro-mobility increases, the R&D related to active safety for micro-mobility is far behind. As a result, we are studying surrounding environmental sensing for micro-mobility, such as environmental map building and moving-object recognition for active safety in sidewalks and streets.

In the case of micro-mobility systems, it is difficult to mount a large number of sensors on the vehicle body, as is the case with cars, because of size and theft concerns. Thus, it is desirable to mount small and easily detachable sensors on the handlebar of the micro-mobility or on the helmet worn by the micro-mobility rider. Our previous work [11] proposed a method of building a 3D point-cloud map in sidewalk and roadway environments using LiDAR attached to the rider's helmet (Helmet-Mounted LiDAR, HML) of a micro-mobility.

This paper presents a SLAMTMO method using HML. The SLAMTMO can not only build a 3D point-cloud map in dynamic and Global Navigation Satellite System (GNSS)-denied environments but also recognize moving objects, such as cars, two-wheelers, and pedestrians. This study is an extension of our previous works [10, 11] on SLAM-based environmental mapping using HML and TMO by motorcycle-mounted LiDAR, and these methods are integrated into our HML system.

Several studies have been accomplished on surrounding environmental sensing using HML. Indoor SLAM, in which people wearing helmets equipped with two-dimensional (2D) LiDAR or one-dimensional (1D) LiDAR walk around in building and factory environments, was presented [12–14]. Niforatos et al. [15] presented a method of skier detection using 1D LiDAR attached to ski helmets to reduce the risk of accidents on ski slopes. To the best of our knowledge, no studies have been conducted on environmental sensing in sidewalks and roadways using 3D LiDAR attached to the rider's helmet of a micro-mobility. Although there have been several studies on helmets with sensors (smart helmets) in the ITS fields [16], their use is limited to alcohol detection in motorcycle riders and collision-accident detection, as well as confirming rider safety after accidents.

 ISBN: 978-1-68558-006-3

The rest of this paper is organized as follows. Section II describes the experimental system. Section III overviews the SLAMTMO. Section IV explains the distortion correction method for the LiDAR scan data, and Section V presents the classification method for scan data related to static and moving objects. Section VI presents experimental results to verify the proposed method, followed by the conclusions and future works in Section VII.

II. Experimental System

Figure 1 shows the overview of the smart helmet. The upper part of the helmet is equipped with a mechanical 64-layer LiDAR (Ouster, OS0-64) and an inertial measurement unit (IMU) (Xsens, MTi-300).

The HML has a maximum range of 55 m, a horizontal field of view of 360 ° with a resolution of 0.35 °, and a vertical field of view of 90 ° with a resolution of 1.4 °. LiDAR can obtain 1024 measurements (distance, direction, and reflected light intensity) every 1.56 ms (every 5.6 ° in the horizontal direction). Therefore, approximately 66,000 points of scan data are acquired in one rotation (360 ° observation) period (100 ms).

Attitude angle (roll and pitch angles) and angular velocity (roll, pitch, and yaw angular velocities) of the helmet are obtained from the IMU every 10 ms. The measurement error for the attitude angle is less than ± 0.3 °, and that of the angular velocity is less than ± 0.2 °/s.

The weight of the mechanical LiDAR is 0.5 kg, and the smart helmet is heavier and larger than usual helmets. Therefore, the LiDAR reduces the usability and practicability of the smart helmet. Moreover, it affects the performance of the helmet in the event of a crash. However, modern LiDAR technology [17] has been developing smaller, more lightweight, and lower power consumption solid-state LiDARs than mechanical LiDARs. The use of solid-state LiDARs will much improve the usability and practicability of the smart helmet.

III. Overview of SLAMTMO

Figure 2 shows the sequence of SLAMTMO. For the environmental mapping and TMO, LiDAR scan data captured in the helmet coordinate system attached to the HML are mapped onto the world coordinate system using the self-pose (3D position and attitude angle) information of the helmet. For this, an accurate self-pose of the helmet is required. NDT-based SLAM [18] is utilized to estimate the self-pose in GNSS-denied environments.

For the i-th measurement point ($i = 1, 2, \ldots n$) in the LiDAR scan data, the position in the helmet coordinate system is denoted by $\boldsymbol{p}_H = (x_H, y_H, z_H)^T$, and that in the world coordinate system by $\boldsymbol{p}_i = (x_i, y_i, z_i)^T$. The following relationship is then represented by the homogeneous transformation:

$$\begin{pmatrix} \boldsymbol{p}_i \\ 1 \end{pmatrix} = \boldsymbol{T}(\boldsymbol{X}) \begin{pmatrix} \boldsymbol{p}_{Hi} \\ 1 \end{pmatrix} \quad (1)$$

where $\boldsymbol{X} = (x, y, z, \phi, \theta, \psi)^T$. $(x, y, z)^T$ and $(\phi, \theta, \psi)^T$ are the 3D position and attitude angle (roll, pitch, and yaw angles), respectively, of the helmet in the world coordinate system. $\boldsymbol{T}(\boldsymbol{X})$ is the following homogeneous transformation matrix:

Figure 1. Overview of the experimental smart helmet.

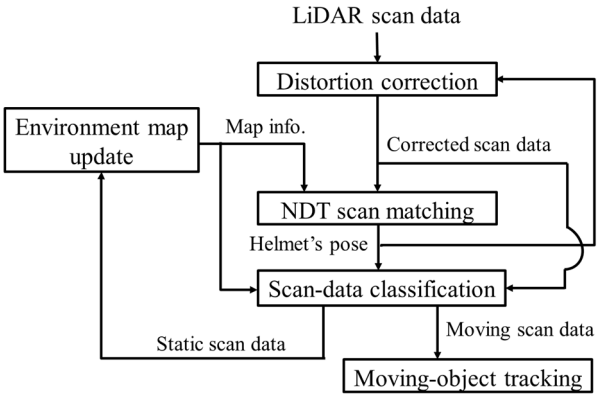

Figure 2. SLAMTMO sequence.

$$\boldsymbol{T}(\boldsymbol{X}) = \begin{pmatrix} \cos\theta\cos\psi & \sin\phi\sin\theta\cos\psi - \cos\phi\sin\psi & \cos\phi\sin\theta\cos\psi + \sin\phi\sin\psi & x \\ \cos\theta\sin\psi & \sin\phi\sin\theta\sin\psi + \cos\phi\cos\psi & \cos\phi\sin\theta\sin\psi - \sin\phi\cos\psi & y \\ -\sin\theta & \sin\phi\cos\theta & \cos\phi\cos\theta & z \\ 0 & 0 & 0 & 1 \end{pmatrix}$$

A voxel map with a cell size of 0.6 m per side is defined in the world coordinate system. In NDT-based SLAM, a normal distributions transformation is performed on the scan data obtained up to the previous time (referred to as environmental map) in each cell of the voxel map, and the mean and covariance of the scan data in each cell are calculated.

The current self-pose (position and attitude angle) $\boldsymbol{X}$ of the helmet is calculated by matching the scan data obtained at the current time (referred to as current scan data) with the environmental map. The current scan data are mapped onto the world coordinate system by performing a coordinate transformation according to (1) using the pose $\boldsymbol{X}$. They are then merged into the environmental map. By repeating this process every LiDAR scan period, the environmental map is built.

The shape of the moving object in TMO is represented by a cuboid with a width W, a length L, and a height H, as shown in Figure 3. The width W_{meas} and length L_{meas} of the moving object are extracted from the scan data related to a moving object (moving scan data). With these values, W and L of the moving object are estimated [10] by

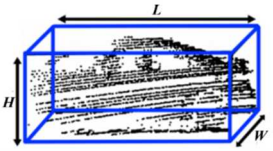

Figure 3. Cuboid around the tracked object (car).

$$\begin{cases} W(t) = W(t-1) + G(W_{meas} - W(t-1)) \\ L(t) = L(t-1) + G(L_{meas} - L(t-1)) \end{cases} \quad (2)$$

where G is the gain.

The height estimate H of the moving object is obtained from the height measurements of the moving scan data.

The Kalman filter is used to estimate the position and velocity of the moving object in the world coordinate system based on the centroid position of the rectangle estimated from (2). When applying the Kalman filter, it is assumed that the object is moving at an approximately constant velocity. In crowded environments, the rule-based data association method [19] is used to accurately match multiple moving objects with multiple moving scan data.

Because LiDAR scans laser in omnidirection, all the scan data within one scan cannot be obtained at a single location when the micro-mobility is moving or swinging, or when the rider's body is swinging. Therefore, if all of the scan data within one scan is transformed using the pose information of the helmet at the same time, distortion arises in the LiDAR scan data mapped in the world coordinate system. Since distortion causes inaccurate results in SLAM and TMO, distortion correction of the LiDAR scan data is required. The distortion-correction method is described in Section IV.

Scan data relating to static and moving objects (static and moving scan data) are used for SLAM and TMO, respectively. For this, accurate classification of static and moving scan data from entire scan data is required. The classification method is described in Section V.

IV. Distortion Correction of LiDAR Scan Data

The helmet's pose is determined every 100 ms (LiDAR scan period) using NDT-based SLAM. The scan data are acquired every 1.56 ms during one rotation of LiDAR. During LiDAR scanning, all the scan data within one scan cannot be obtained at a single location when the micro-mobility is moving or swinging, or when the rider's body is swinging. If all the scan data within one scan is transformed using the pose information of the helmet at the same time, distortion appears in the mapping of the LiDAR scan data onto the world coordinate system. Therefore, the distortion in the scan data is corrected by estimating the helmet's pose using the extended Kalman filter (EKF) every 1.56 ms, i.e., every LiDAR scan data are obtained.

In the EKF for correcting the scan-data distortion, a constant velocity model is used as the helmet motion. As shown in Figure 4, the translational velocity of the helmet in the helmet coordinate system (O_H-$x_Hy_Hz_H$) is denoted by (V_x, V_y, V_z), and the angular velocity (roll, pitch, and yaw angular velocities) by $(\dot{\phi}_H, \dot{\theta}_H, \dot{\psi}_H)$. The following motion model of the helmet can be obtained assuming that the helmet moves at nearly constant translational and angular velocities:

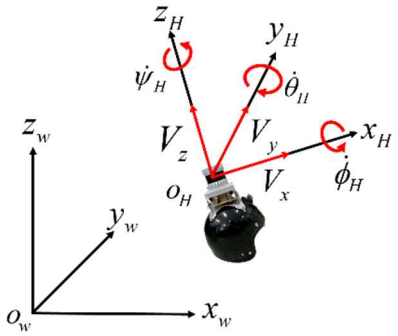

Figure 4. Notation related to the helmet motion.

$$\begin{pmatrix} x_{(t+1)} \\ y_{(t+1)} \\ z_{(t+1)} \\ \phi_{(t+1)} \\ \theta_{(t+1)} \\ \psi_{(t+1)} \\ V_{x(t+1)} \\ V_{y(t+1)} \\ V_{z(t+1)} \\ \dot{\phi}_{H(t+1)} \\ \dot{\theta}_{H(t+1)} \\ \dot{\psi}_{H(t+1)} \end{pmatrix} = \begin{pmatrix} x_{(t)} + a_{1(t)}\cos\theta_{(t)}\cos\psi_{(t)} \\ \quad + a_{2(t)}\{\sin\phi_{(t)}\sin\theta_{(t)}\cos\psi_{(t)} - \cos\phi_{(t)}\sin\psi_{(t)}\} \\ \quad + a_{3(t)}\{\cos\phi_{(t)}\sin\theta_{(t)}\cos\psi_{(t)} + \sin\phi_{(t)}\sin\psi_{(t)}\} \\ y_{(t)} + a_{1(t)}\cos\theta_{(t)}\sin\psi_{(t)} \\ \quad + a_{2(t)}\{\sin\phi_{(t)}\sin\theta_{(t)}\sin\psi_{(t)} + \cos\phi_{(t)}\cos\psi_{(t)}\} \\ \quad + a_{3(t)}\{\cos\phi_{(t)}\sin\theta_{(t)}\sin\psi_{(t)} - \sin\phi_{(t)}\cos\psi_{(t)}\} \\ z_{(t)} - a_{1(t)}\sin\theta_{(t)} + a_{2(t)}\sin\phi_{(t)}\cos\theta_{(t)} \\ \quad + a_{3(t)}\cos\phi_{(t)}\cos\theta_{(t)} \\ \phi_{(t)} + a_{4(t)} + \{a_{5(t)}\sin\phi_{(t)} + a_{6(t)}\cos\phi_{(t)}\}\tan\theta_{(t)} \\ \theta_{(t)} + \{a_{5(t)}\cos\phi_{(t)} - a_{6(t)}\sin\phi_{(t)}\} \\ \psi_{(t)} + \{a_{5(t)}\sin\phi_{(t)} + a_{6(t)}\cos\phi_{(t)}\}\dfrac{1}{\cos\theta_{(t)}} \\ V_{x(t)} + \tau w_{\dot{V}x} \\ V_{y(t)} + \tau w_{\dot{V}y} \\ V_{z(t)} + \tau w_{\dot{V}z} \\ \dot{\phi}_{H(t)} + \tau w_{\ddot{\phi}_H} \\ \dot{\theta}_{H(t)} + \tau w_{\ddot{\theta}_H} \\ \dot{\psi}_{H(t)} + \tau w_{\ddot{\psi}_H} \end{pmatrix} \quad (3)$$

where (x, y, z) and (ϕ, θ, ψ) are the position and attitude angle (roll, pitch, and yaw angles), respectively, of the helmet in the world coordinate system (O_w-$x_wy_wz_w$). $(w_{\dot{V}x}, w_{\dot{V}y}, w_{\dot{V}z}, w_{\ddot{\phi}_H}, w_{\ddot{\theta}_H}, w_{\ddot{\psi}_H})$ is the acceleration disturbance. τ is the LiDAR scan period. $a_1 = V_x\tau + \tau^2 w_{\dot{V}x}/2$, $a_2 = V_y\tau + \tau^2 w_{\dot{V}y}/2$, $a_3 = V_z\tau + \tau^2 w_{\dot{V}z}/2$, $a_4 = \dot{\phi}_H\tau + \tau^2 w_{\ddot{\phi}_H}/2$, $a_5 = \dot{\theta}_H\tau + \tau^2 w_{\ddot{\theta}_H}/2$, and $a_6 = \dot{\psi}_H\tau + \tau^2 w_{\ddot{\psi}_H}/2$.

Figure 5 shows the sequence of distortion correction. The LiDAR scan period (100 ms) is denoted as τ, the IMU observation period (10 ms) as $\Delta\tau_{IMU}$, and the scan data observation period (1.56 ms) as $\Delta\tau$. Here, the method for correcting the scan-data distortion obtained between time $(t-1)\tau$ and $t\tau$ is described [20].

Let us suppose that at the time $(t-1)\tau$, the pose of the helmet is calculated by NDT-based SLAM and estimated via EKF. The IMU data are obtained 10 times per LiDAR scan ($\tau = 10\Delta\tau_{IMU}$). Using the IMU data obtained every $\Delta\tau_{IMU}$, the EKF

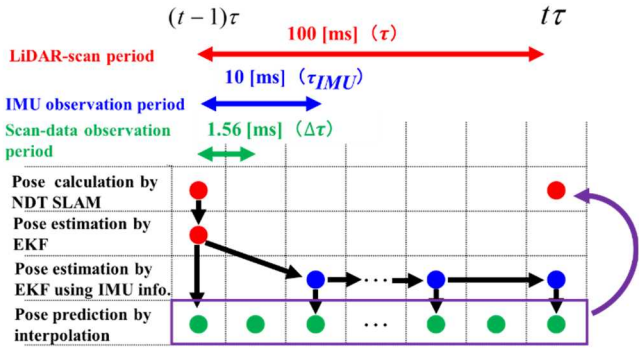

Figure 5. Sequence of distortion correction.

estimates the pose $\hat{\boldsymbol{X}}(t-1,k)$ at the time $(t-1)\tau + k\Delta\tau_{IMU}$, where k = 0–10. Since the observation period $\Delta\tau_{IMU}$ of the IMU is 10 ms, and the scan-data observation period $\Delta\tau$ is 1.56 ms, the LiDAR scan data are obtained six times within the IMU observation period ($\Delta\tau_{IMU} = 6\Delta\tau$).

From the estimates, $\hat{\boldsymbol{X}}(t-1,k)$ at the time $(t-1)\tau + k\Delta\tau_{IMU}$ and $\hat{\boldsymbol{X}}(t-1,k+1)$ at $(t-1)\tau + (k+1)\Delta\tau_{IMU}$ the interpolation algorithm predicts the helmet's pose $\hat{\boldsymbol{X}}(t-1,k,j)$ at $(t-1)\tau + k\Delta\tau_{IMU} + j\Delta\tau$ (where j = 1–5), at which the scan data are acquired.

The scan data $\boldsymbol{p}_{Hi}(t-1,k,j)$ (where i = 1, 2, …, n) obtained at $(t-1)\tau + k\Delta\tau_{IMU} + j\Delta\tau$ in the helmet coordinate system are transformed to $\boldsymbol{p}_i(t-1,k,j)$ in the world coordinate system using Eq. (1) as follows:

$$\begin{pmatrix} \boldsymbol{p}_i(t-1,k,j) \\ 1 \end{pmatrix} = \boldsymbol{T}(\hat{\boldsymbol{X}}(t-1,k,j)) \begin{pmatrix} \boldsymbol{p}_{Hi}(t-1,k,j) \\ 1 \end{pmatrix} \quad (4)$$

Using the pose estimate $\hat{\boldsymbol{X}}(t-1,10)$ at $t\tau$ (= $(t-1)\tau + 10\Delta\tau_{IMU}$), the scan data $\boldsymbol{p}_i(t-1,k,j)$ obtained by Eq. (4) is again transformed into the scan data $\boldsymbol{p}^*_{Hi}(t)$ in the helmet coordinate system at $t\tau$ by

$$\begin{pmatrix} \boldsymbol{p}^*_{Hi}(t) \\ 1 \end{pmatrix} = T(\hat{\boldsymbol{X}}(t-1,10))^{-1} \begin{pmatrix} \boldsymbol{p}_i(t-1,k,j) \\ 1 \end{pmatrix} \quad (5)$$

$\boldsymbol{p}^*_{Hi}(t)$ is the scan data that correct distortion at $t\tau$. Using the corrected scan data, SLAMTMO is performed.

V. Classification of Static and Moving Scan Data

For SLAM, the moving scan data have to be eliminated and the static scan data have to be extracted from the whole LiDAR scan data. TMO conversely requires the removal of static scan data and the extraction of moving scan data from the whole LiDAR scan data. For this, accurate classification of static and moving scan data is required. Although the classification is usually performed based on the occupancy grid method, in practical environments, LiDAR noises and outliers frequently cause misclassification.

We utilize an environment map built by NDT-based SLAM to minimize the misclassification. We call this approach environment map subtraction (EMS)-based classification or dynamic background subtraction-based method [10]. Figure 6 shows the EMS-based classification method. In this method, we subtract the environment map built by NDT-based SLAM from the current scan data to remove as much static scan data as possible from the entire LiDAR scan data. The scan data extracted using the EMS-based method are mapped onto a grid map. The cell on the grid map is a square with a side-length of 0.3 m. A cell in which scan data exist is called an occupied cell. For the moving scan data, the time to occupy the same cell is short (less than 0.7 s in this paper), whereas for the static scan data, the time is long (not less than 0.7 s). Therefore, by using the occupancy grid method based on the cell occupancy time [19], cells occupied by moving scan data (or static scan data) can be detected as moving cells (or static cells).

Because an object takes multiple cells, adjacent occupied cells are clustered. Then, clustered moving cells (or static cells) are obtained as a moving cell group (or static cell group). The scan data contained in the moving cell group are finally decided as the moving scan data. The static scan data are extracted by subtracting the moving scan data from the LiDAR current scan data.

The LiDAR field of view also moves along with the micro-mobility movement. Even though an object that recently enters the LiDAR field of view is static, it is misclassified as a moving object because the cell occupancy time is short. To address this problem, new-observation cells are defined on the grid map, which correspond to the new field of view of the LiDAR. The time of cells entering the LiDAR field of view (T_{NC}) and the cell occupancy time (T_{OC}) are measured, and the occupancy time rate (α) is calculated by $\alpha = T_{OC} / T_{NC}$. Cells in which α is 10% or more are determined to be new-observation cells and then considered moving cells. This can minimize the false classification of static objects recently entering the LiDAR field of view as moving objects.

The scan data in the environment map are sparser in the areas in front of the micro-mobility and in the occlusion areas. Therefore, the static scan data likewise exist in a sparse state

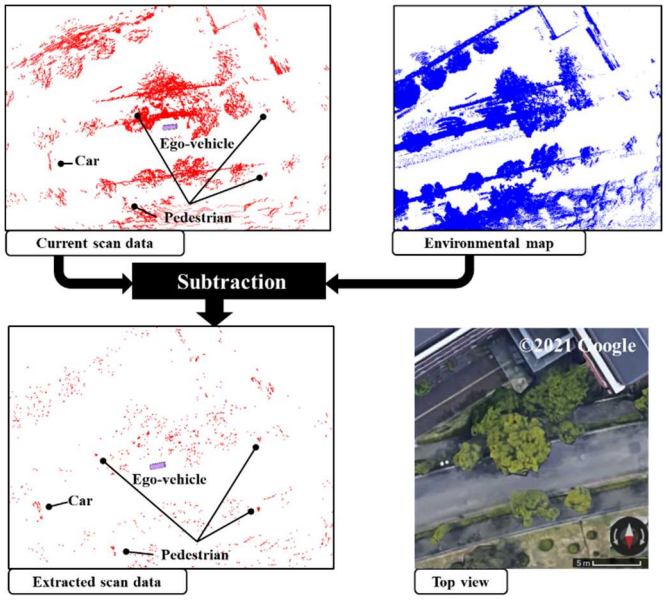

Figure 6. Sequence of EMS-based classification (top view).

when the environment map is subtracted from the current scan data. If the scan data, sparsely extracted based on the EMS-based method, are mapped onto a grid map, it may be erroneously determined as a moving cell.

To overcome this issue, the scan data removed by the EMS-based method are additionally mapped onto the grid map as static cells. As a result, sparse static scan data that tend to be moving cells and static scan data that are removed by the EMS-based method are both mapped onto the grid map. Neighboring cells, in which these static scan data are occupied, are clustered, and the cell group is then determined to be a static cell group. Accordingly, sparse static scan data are correctly determined as static scan data by the occupancy grid method.

VI. Fundamental Experiments

A micro-mobility was moved on our university-campus road, as shown in Figure 7, and SLAMTMO is performed. The traveling distance of the mobility is approximately 500 m, and the maximum speed is approximately 30 km/h. Figure 8 shows the attitude angle and angular velocity of the helmet during driving, which are observed by the IMU.

Figure 8 shows the TMO results. In Figure 9(b), the blue rectangle indicates the assessed size of the moving object, and the blue stick indicates the moving direction of the moving object obtained from the velocity estimate. The black (or red) dots reveal the scan data removed (or extracted) from the LiDAR scan data using the EMS-based method.

The micro-mobility is moved three times along the path shown in Figure 7 (a). Then, 111 moving objects (106 pedestrians and five cars) are tracked. The TMO performance is examined under the following two cases:

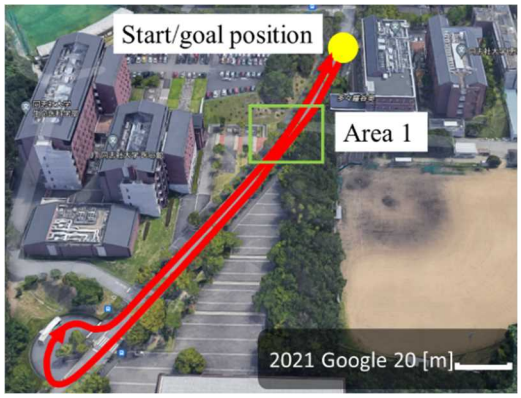

(a) Top view

(b) Side view

Figure 7. Photo of experimental environment.

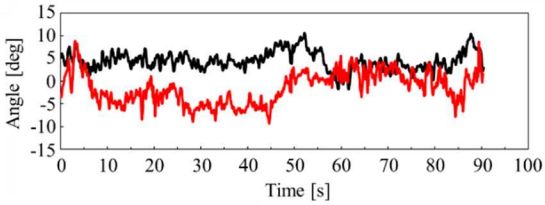

(a) Roll (black) and Pitch(red) angles

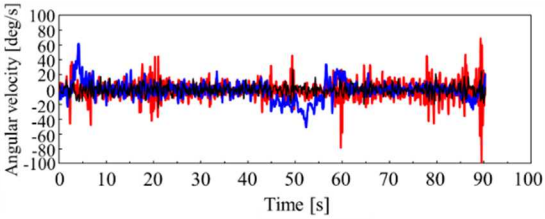

(b) Roll (black), pitch (red) and yaw (blue) angular velocities

Figure 8. Attitude angle and angular velocity of helmet.

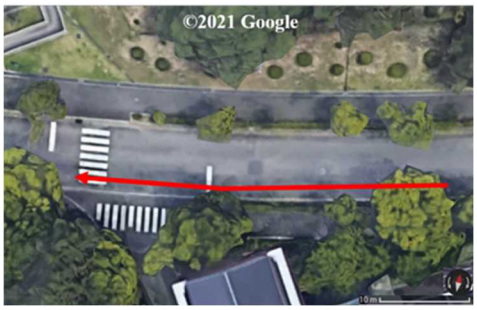

(a) Photo of area 1

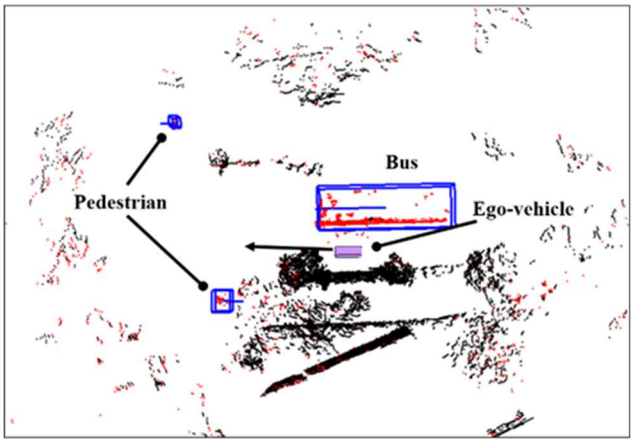

(b) Estimated track and size of the moving objects in area 1

Figure 9. Tracking result (top view).

・Case 1: Tracking with distortion correction of LiDAR scan data and EMS-based classification method (proposed method)

・Case 2: Tracking without using either method.

As the result, in case 1, 109 objects (104 pedestrians and five cars) can be successfully tracked, and two pedestrians cannot be tracked. In case 2, conversely, 103 objects (98 pedestrians and five cars) can be successfully tracked, and eight

 ISBN: 978-1-68558-006-3

pedestrians cannot be tracked. Pedestrians who are not being tracked are mistakenly classified as static objects. From these results, our proposed method gives better TMO accuracy.

Figure 10 shows the SLAM result estimated by the proposed method (case 1). In the SLAM, the mapping accuracy can be evaluated by the pose accuracy. Therefore, the error of position estimate of the helmet at the goal position is measured by a GNSS/LiDAR positioning system set at the goal position. Table I reveals the result, in which the micro-mobility is moved three times on the road shown in Figure 7. From the table, the proposed method (case 1) provides the SLAM accuracy better than case 2.

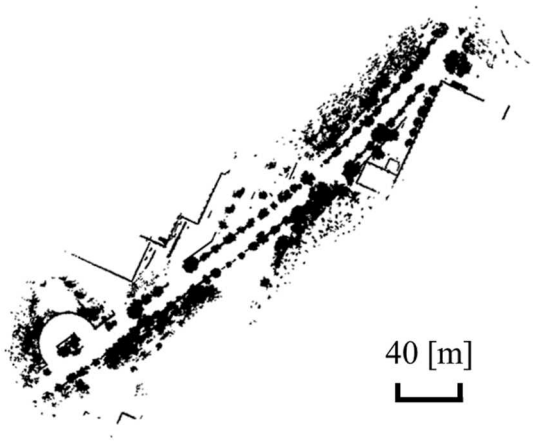

(a) Overall map (top view)

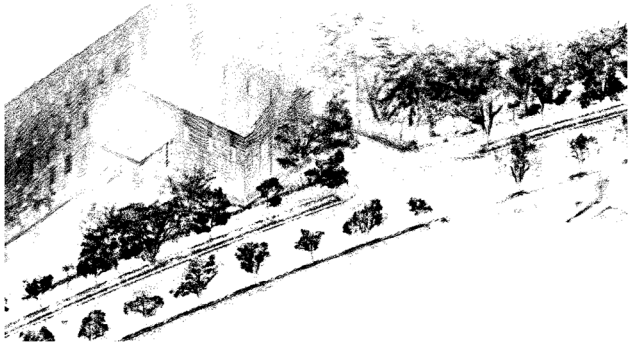

(b) Map in area 1 (bird's-eye view)

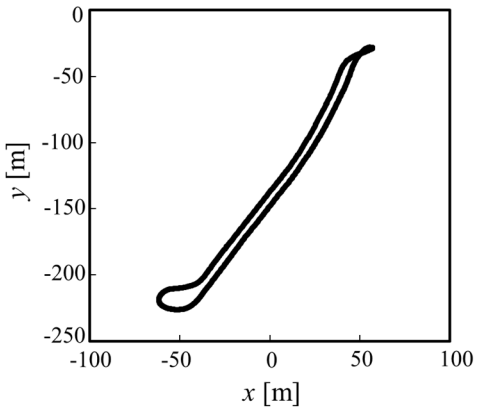

(c) Position estimate

Figure 10. SLAM result.

TABLE I. ERROR OF POSITION ESTIMATE OF HELMET AT GOAL POSITION.

	Case 1	Case 2
Exp 1	0.23 m	5.91 m
Exp 2	1.93 m	15.10 m
Exp 3	0.71 m	6.03 m

TABLE II. PROCESSING TIME OF SLAMTMO (CASE 1)

	Distortion correction and NDT SLAM	Scan data classification	Environment map update, moving-object tracking, and others	Total
Exp 1	2180 ms	801 ms	33 ms	3014 ms
Exp 2	2068 ms	719 ms	30 ms	2817 ms
Exp 3	1815 ms	659 ms	33 ms	2507 ms
Mean	2021 ms	726 ms	32 ms	2779 ms

TABLE III. PROCESSING TIME OF SLAMTMO (CASE 2)

	NDT SLAM	Scan data classification	Environment map update, moving-object tracking, and others	Total
Exp 1	1753 ms	242 ms	23 ms	2025 ms
Exp 2	1832 ms	285 ms	27 ms	2144 ms
Exp 3	1713 ms	239 ms	25 ms	1977 ms
Mean	1766 ms	255 ms	27 ms	2049 ms

In the experiments, LiDAR scan data are recorded, and SLAMTMO is executed offline by a computer. The specifications of the computer are as follows: Windows 10 Pro OS, Intel(R) Core (TM) i7-1065G7 @1.30GHz CPU, 16 GB RAM, and C++ software language. The point cloud library (PCL) [21] is used for NDT-based SLAM. Tables II and III show the processing time of SLAMTMO in cases 1 and 2, respectively.

Although long computational time is currently required, as shown in Tables II and III, the computational time can be reduced by optimizing the program code and using a graphical processing unit for real-time operations.

VII. CONCLUSIONS

This paper presented a SLAMTMO method in dynamic and GNSS-denied environments utilizing LiDAR attached to a helmet worn by a rider of micro-mobility (helmet-mounted LiDAR). To accurately perform environmental mapping and TMO, the distortion of scanning LiDAR data was corrected using the self-pose information by NDT-based SLAM and IMU information via EKF. Furthermore, static and moving scan data were classified by the EMS-based classification and occupancy grid-based methods. The performance of the presented method was examined through experiments in a road environment of our university campus.

Experiments in various sidewalk and roadway situations are now being carries out to thoroughly evaluate the proposed

 ISBN: 978-1-68558-006-3

method. In future works, we will detect obstacles on road surfaces, such as curbs, gutters, and steps, using LiDAR and accelerometer to reduce the falling risk of micro-mobility. Additionally, we will include the obstacle information in the environment map.

REFERENCES

[1] E. Yurtsever, J. Lambert, A. Carballo, and K. Takeda, "A Survey of Autonomous Driving: Common Practices and Emerging Technologies," IEEE Access, vol. 8, pp. 58443–58469, 2020.

[2] N. Boysen, S. Fedtke, and S. Schwerdfeger, "Last-Mile Delivery Concepts: A Survey from an Operational Research Perspective," OR Spectrum, vol. 43, pp. 1–58, 2021.

[3] B. Huang, J. Zhao, and J. Liu, "A Survey of Simultaneous Localization and Mapping," eprint arXiv:1909.05214, 2019.

[4] S. Kuutti et al., "A Survey of the State-of-the-Art Localization Techniques and Their Potentials for Autonomous Vehicle Applications," IEEE Internet of Things Journal, vol.5, pp. 829–846, 2018.

[5] A. Mukhtar, L. Xia, and TB. Tang, "Vehicle Detection Techniques for Collision Avoidance Systems: A Review," IEEE Trans. on Intelligent Transportation Systems, vol. 16, pp. 2318–2338, 2015.

[6] E. Marti, J. Perez, MA. Miguel, and F. Garcia, "A Review of Sensor Technologies for Perception in Automated Driving," IEEE Intelligent Transportation Systems Magazine, pp. 94–108, 2019.

[7] S. Tanaka, C. Koshiro, M. Yamaji, M. Hashimoto, and K. Takahashi, "Point Cloud Mapping and Merging in GNSS-Denied and Dynamic Environments Using Only Onboard Scanning LiDAR," Int. J. on Advances in Systems and Measurements, vol. 13, pp. 275–288, 2020.

[8] K. Matsuo, A. Yoshida, M. Hashimoto, and K. Takahashi, "NDT Based Mapping Using Scanning Lidar Mounted on Motorcycle," Proc. of the Fifth Int. Conf. on Advances in Sensors, Actuators, Metering and Sensing, pp. 69–75, 2020.

[9] S. Sato, M. Hashimoto, M. Takita, K. Takagi, and T. Ogawa, "Multilayer Lidar-Based Pedestrian Tracking in Urban Environments," Proc. of IEEE Intelligent Vehicles Symp., pp. 849–854, 2010.

[10] S. Muro, I. Yoshida, M. Hashimoto, and K. Takahashi, "Moving-Object Tracking by Scanning LiDAR Mounted on Motorcycle Based on Dynamic Background Subtraction," Artificial Life and Robotics, vol. 26, issue 4, pp. 412–422, 2021.

[11] A.Yoshida, I. Yoshida, M. Hashimoto, and K. Takahashi, "Point-Cloud Mapping by Helmet-Mounted LiDAR Based on NDT SLAM," Proc. of 23rd IEEE Int. Conf. on Industrial Technology, 2022, to be presented.

[12] Y. Cai, S. Hackett, G., Ben, F. Alber, and S. Mel, "Heads-Up Lidar Imaging with Sensor Fusion," Electronic Imaging, The Engineering Reality of Virtual Reality 2020, pp. 338-1–338-7, 2020.

[13] B. Cinaz and H. Kenn, "Head SLAM - Simultaneous Localization and Mapping with Head-Mounted Inertial and Laser Range Sensors," Proc. of 12th IEEE Int. Symp. on Wearable Computers, 2008.

[14] H. Sadruddin, A. Mahmoud, and M. M. Atia, "Enhancing Body-Mounted LiDAR SLAM using an IMU-based Pedestrian Dead Reckoning (PDR) Model," Proc. of 2020 IEEE 63rd Int. Midwest Symp. on Circuits and Systems, 2020.

[15] E. Niforatos, I. Elhart, A. Fedosov, and M. Langheinrich, " s-Helmet: A Ski Helmet for Augmenting Peripheral Perception," Proc. of the 7th Augmented Human Int. Conf.,2016.

[16] A. Pangestu, M. N. Mohammed, S. Al-Zubaidi, S. H. K. Bahrain, and A. Jaenul, "An Internet of Things Toward a Novel Smart Helmet for Motorcycle: Review," AIP Conf. Proceedings 2320, 050026, 2021.

[17] T. Raj, F. H. Hashim, A. B. Huddin, M. F. Ibrahim, and A. Hussain, "A Survey on LiDAR Scanning Mechanisms," Electronics, 2020.

[18] P. Biber and W. Strasser, "The Normal Distributions Transform: A New Approach to Laser Scan Matching," Proc. of IEEE/RSJ Int. Conf. on Intelligent Robots and Systems, pp. 2743–2748, 2003.

[19] M. Hashimoto, S. Ogata, F. Oba, and T. Murayama, "A Laser Based Multi-Target Tracking for Mobile Robot," Intelligent Autonomous Systems 9, pp. 135–144, 2006.

[20] K. Tokorodani, M. Hashimoto, Y. Aihara, and K. Takahashi, "Point-Cloud Mapping Using Lidar Mounted on Two-Wheeled Vehicle Based on NDT Scan Matching," Proc. of the 16th Int. Conf. on Informatics in Control, Automation and Robotics, pp. 446–452, 2019.

[21] R. B. Rusu and S. Cousins, "3D is here: Point Cloud Library (PCL)," Proc. of 2011 IEEE Int. Conf. on Robotics and Automation, 2011.

 ISBN: 978-1-68558-006-3